한국동력기계공학회지 제17권 제5호 pp. 23-29 2013년 10월 (ISSN 1226-7813)
Journal of the Korean Society for Power System Engineering, Vol. 17, No. 5, pp. 23-29, October 2013
Research paper

The Structural Characterization of Pristine and Ground Graphenes with Different Grinding Speed in Planetary Ball Mill

Tae-Jin Lee*, Myekhlai Munkhshur**, Md. Riyad Tanshen**, Dae-Chul Lee**, Han-Shik Chung*** and Hyo-Min Jeong***

(received 21 august 2013, revised 02 September 2013, accepted 02 September 2013)

Abstract : The activation process is the key to graphene's practical application. In this study, the effect of grinding speed in planetary ball mill on structural integrity of graphene has been studied at various grinding speed such as 100 rpm, 200 rpm, 300 rpm, 400 rpm and 500 rpm. The morphology and structure of pristine graphene and ground graphenes were studied using scanning electron microscopy (SEM), transmission electron microscopy (TEM), X–ray diffraction (XRD) and Raman spectroscopy respectively. According to these results, structural properties of graphene were improved when grinding speed was increased.

Key Words : Pristine Graphene, Ground graphene, Grinding speed

1. Introduction

Graphene (GN), a single-atom-thick sheet of hexagonally arrayed sp^2-bonded carbon atoms, have attracted much attention in recent years due to their extraordinary features such as excellent thermal and electrical conductivity, high values of mechanical stiffness, optical transmittance, specific surface area and strong catalytic activity[1~5]. Because of these properties, GN have a wide range of applications including transparent conductive films, organic photovoltaic (PV) cells, field effect transistor devices, ultrasensitive sensors, polymer composite materials, electromechanical systems, hydrogen storage, energy conversion and storage, batteries, solar cells and drug delivery systems[6~9].

The use of pristine GN in nano device is not suitable for practical application due to GN tend to agglomerate and restack through - and van der Waals interactions resulting indigent dispersion and inferior properties. Surface modification of GN is the potential solution to overcome van der Waals force. The ball milling process is widely used for decreasing agglomeration and restacking process of nanostructured carbons[10~12].

In this study ball milling process was used for diminish agglomeration and restacking process of GN in order to improve a dispersion and special properties of GN. The aim of present work is to study the influence of grinding speed in planetary

*Tae-Jin Lee(corresponding author) : Department of Mechanical and Energy Engineering, Gyeongsang National University.
E-mail : hansumguy1@nate.com
**Myekhlai Munkhshur, Md. Riyad Tanshen and Dae-Chul Lee : Department of Mechanical and Energy Engineering, Gyeongsang National University.
***Han-Shik Chung and Hyo-Min Jeong : Department of Mechanical and Energy Engineering, Gyeongsang National University Institute of Marine Industry.

ball mill on special properties of GN.

2. Experimental Details

2.1 Preparation of the Ground Structures GN

GN (AO-2) with a specific surface area (SSA) of 100 m^2*g^{-1} and 99.2% purity (purchased from Graphene Supermarket, USA) was used as the GN source.

The planetary ball mill (HPM-700) (Haji Engineering, Korea) was used to grind the sample. Grinding process was carried out at different grinding speed such as 100 rpm, 200 rpm, 300 rpm, 400 rpm and 500 rpm as following literature [12].

Ultrasonication 1510E–DTH (Branson Ultrasonic Corporation, USA) was used for preparation GN suspension.

2.2 Characterization of pristine GN and ground GNs

Morphological characteristics of the pristine GN and ground GNs were carried out by scanning electron microscopy (SEM) (JSM-6710F, JEOL) and transmission electron microscopy (TEM) (JEM-2100F, JEOL).

Particle size of pristine and ground GNs was determined using Particle size analyzer (Malvern, Zetasizer Nano–S90).

X–ray diffraction (XRD) (D8 advance powder diffraction, Bruker AXS) using Cu K_α radiation (λ =1.5406 Å) was used to study crystal structure of pristine and ground graphenes. The samples were rotated at 10 rpm and swept from 2=10 through to 90 using default parameters of program of the diffraction that was equipped with Bruker AXS Diffrac PLUS software. The GN distance layer can be calculated based on Bragg's law[13~14]:

$$n\lambda = 2d_{(hkl)}\sin(\theta) \quad (1)$$

where is the wavelength of the X–ray, is the scattering angle, n is an integer representing the order of the diffraction peak, d is the interplane distance of the lattices and (hkl) are Miller indices. The well–known Debye Scherrer equation can obtain the mean crystallite size of power composed of relatively perfect crystalline particle [13~14]:

$$L_{hkl} = \frac{k\lambda}{\beta_0 \cos\theta} \quad (2)$$

where Lhkl is the mean dimension of the crystallite perpendicular to the plane (hkl), $_o$ is the integral full width half maximum in radians, K is a constant dependent on the crystallite shape (0.89).

The number of graphene layers (N) can be obtained using the following equation[13~14]:

$$N = \frac{L_{hkl}}{d_{hkl}} \quad (3)$$

Structural changes were studied by Labram HR800 Raman spectrometer with a 514 nm Argon ion laser operating at Raman shift ranging from 1200 to 1700 cm^{-1}.

3. Results and Discussion

SEM and TEM were used to detect possible morphological changeson pristine GN and ground GNs specimens depending on the grinding speed. Fig. 1 shows SEM micrographs of pristine GN and ground GNs. As shown in Fig. 1a, morphology of pristine GN is rough and dispersion is not good. After grinding process with different grinding speed such as 100 rpm (GN100), 200 rpm (GN200), 300 rpm (GN300), 400 rpm (GN400) and 500 rpm (GN500) (Fig. 1b-1f), ground GNs surface was getting homogeneous and good dispersibility was occurred with increasing the grinding speed. It means that all GNs were broken and particle size of GNs was decreased.

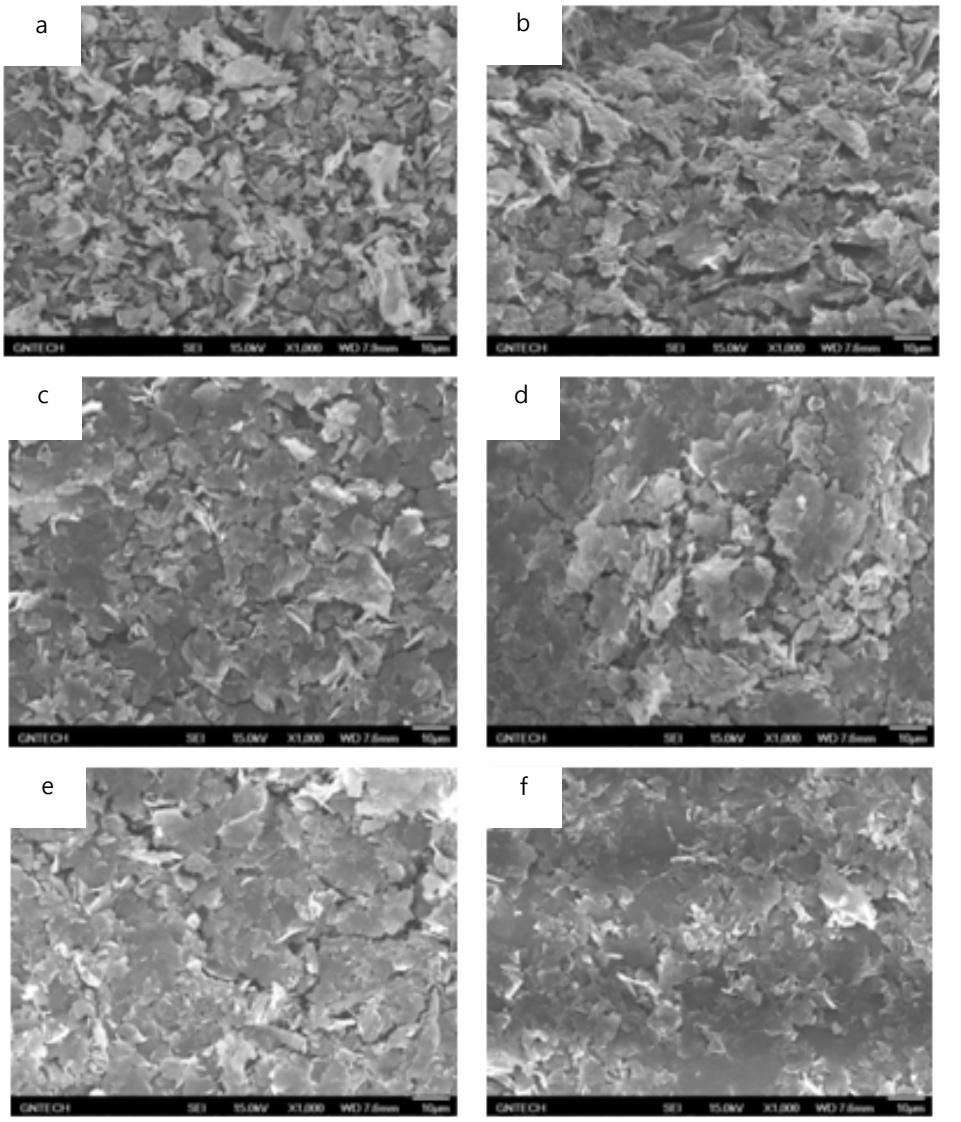

Fig. 1 SEM micrographs of GNs: (a) Pristine GN, (b) GN100, (c) GN200, (d) GN300, (e) GN400 and (f) GN500

The TEM images of pristine GN as well ground GNs with different grinding speed at 100 rpm, 200 rpm, 300 rpm, 400 rpm and 500 rpm are presented in Fig. 2. From TEM image of pristine GN (Fig. 2a), particles of GN were more agglomerated. The agglomeration of ground GNs particles was decreased in Fig. 2b–2f with increasing grinding speed. Agglomeration of GN400 and GN500 was decreased significantly due to particle size was decreased.

The average particle size of pristine and ground GNs was determined using particle size analyzer. Fig. 3 shows average particle size of pristine GN and ground GNs. The average particle size of GN was significantly decreased with increasing the ground speed due to the high energy grinding

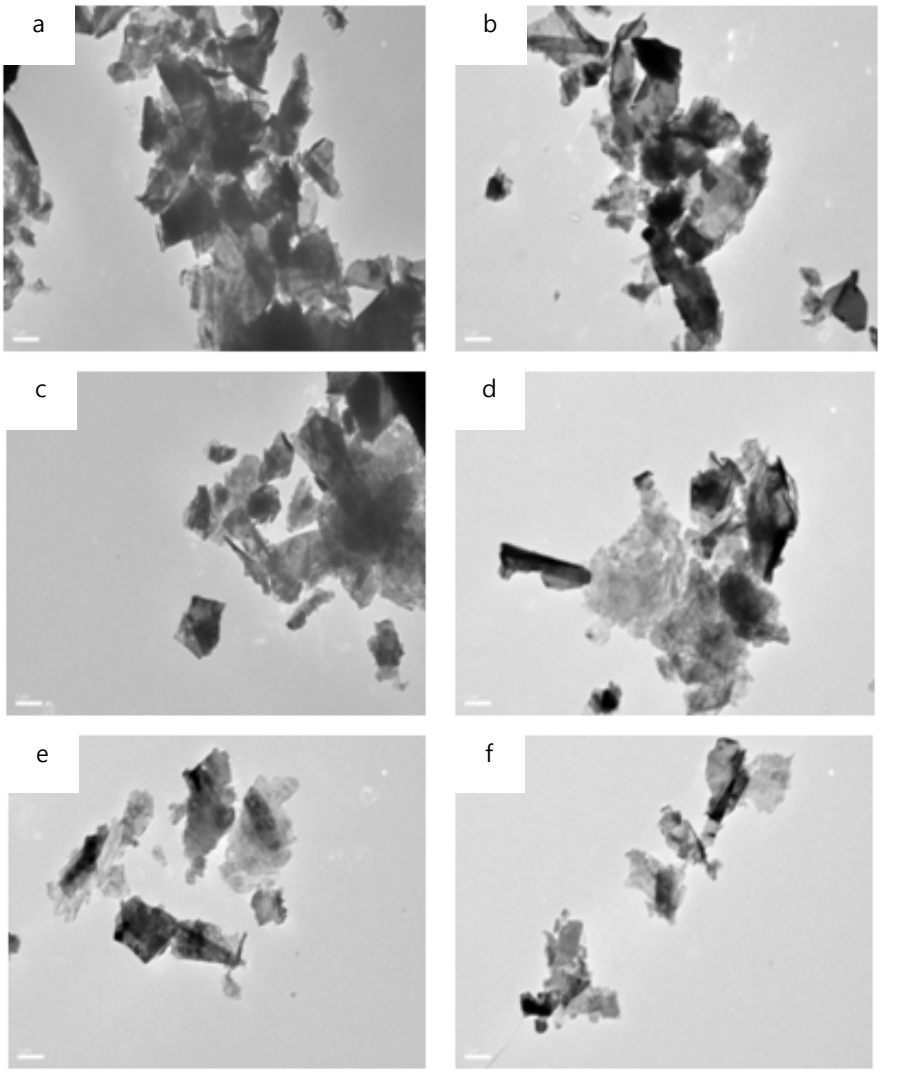

Fig. 2 TEM images of GNs: (a) Pristine GN, (b) GN100, (c) GN200, (d) GN300, (e) GN400 and (f) GN500

process.

Crystal structure of pristine and ground GNs was studied by XRD whereas the layer distance, crystal thickness and number of layer were determined by Bragg's law and Debye Scherrer equation (eq. (1), (2) and (3)) from XRD pattern (Table 1). The XRD patterns of pristine and ground GNs are shown in Fig. 4. The (002), (101), (004), (110) and (112) peaks of crystal and amorphous GN were detected in XRD pattern of pristine GN (Fig. 4a). In XRD patterns of GN100 and GN200 some peaks were disappeared. And, only (002) and (004) peaks of crystal GN were observed in XRD patterns of GN300, GN400 and GN500. On the other hand number of peak was decreased and XRD patterns were changed to more cleanly when grinding speed was increased. From XRD results, ground speed of ball milling process is not influenced for layer

distance, crystal thickness and number of layer but ground speed of ball milling process is effectively influenced for crystallinity of GN. Crystal structure of GN was existed more crystallinity and homogenously when grinding speed is increased.

Raman spectroscopy is powerful tool for investigating the order/disorder structure of carbon material. Fig. 5 shows the Raman spectroscopy of pristine and ground GNs. The Raman spectrum of

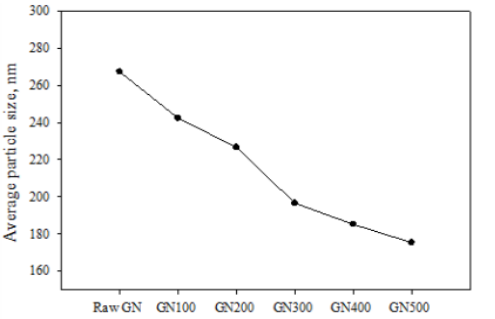

Fig. 3 Average particle size of GNs

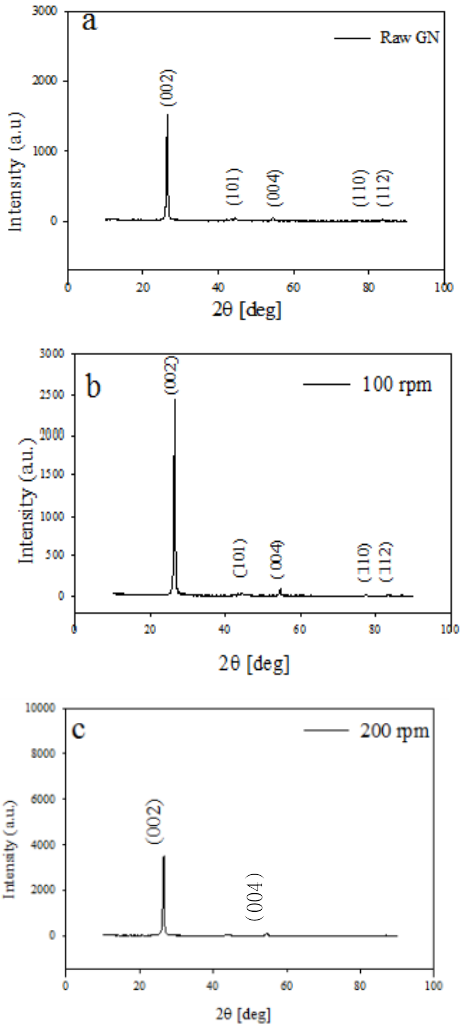

Fig. 3 XRD patterns of Graphenes a. Pristine graphene b. GN100 c. GN200

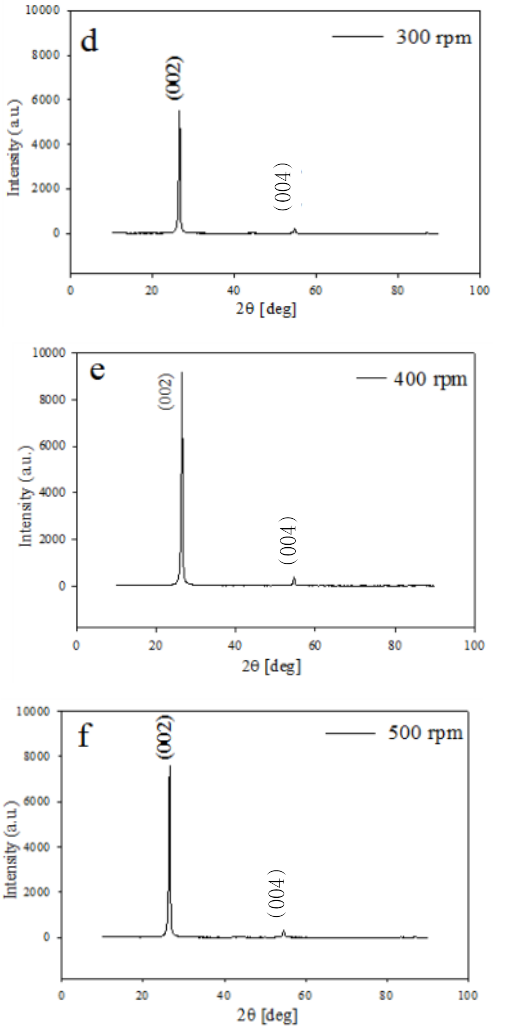

Fig. 3 XRD patterns of Graphenes d. GN300 e. GN400 f. GN500

Table 1 X - ray structural parameters of pristine and ground graphenes

Sample	2Θ	FWHM(°)	Layer distance (Å)	Crystral thickness (nm)	Number of layers
Pristine GN	26.50	0.40	~3.36	~20.0	~60.0
GN100	26.50	0.40	~3.36	~20.0	~60.0
GN200	26.54	0.40	~3.36	~20.0	~60.0
GN300	26.56	0.40	~3.36	~20.0	~60.0
GN400	26.54	0.40	~3.36	~20.0	~60.0
GN500	26.52	0.40	~3.36	~20.0	~60.0

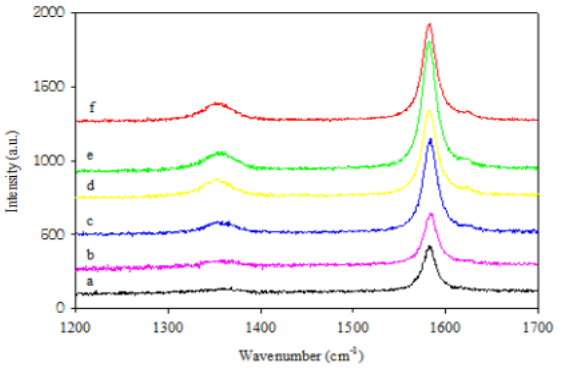

Fig. 5 Raman spectroscopy of graphenes a. pristine graphene, b. GN100, c. GN200, d. GN300, e. GN400 and f. GN500

the GNs includes both G (1580 cm^{-1}) and D (1353 cm^{-1}) bands, which are attributed to disorder induced and tangential mode peaks, respectively.

The intensity ratio (I_D/I_G) of the D and G bands of raw and ground GN (Table 2) was decreased when grinding speed is decreased, which indicates of the amount of carbon defects sites.

On the other hand, structural defect and disorder were decreased while the structure of graphene particles become more homogeneously when grinding speed is increased. Small intensity ratio indicates good crystallinity of GN[15].

Table 2 Intensity ratio (ID/IG) of the D and G bands of raw and ground GNs

Samples	Pristine GN	GN100	GN200
Intensity ratio (I_D/I_G)	0.320	0.320	0.277
Samples	GN300	GN400	GN500
Intensity ratio (I_D/I_G)	0.263	0.262	0.221

5. Conclusions

In this work an influence of grinding speed in planetary ball mill on the specific properties of graphene was studied. Ball mill process was carried out at different grinding speed such as 100 rpm, 200 rpm, 300 rpm, 400 rpm and 500 rpm.

- Morphological characteristic was more homogenously and with high dispersion for increasing speed due to particle size was decreased.
- From XRD results, ground speed of ball milling process is not influenced for layer distance, crystal thickness and number of layer but ground speed of ball milling process is effectively influenced for crystallinity of graphene. Crystal structure of graphene was existed more crystallinity and homogenously when grinding speed is increased.
- The structural defect and disorder were decreased while the structure of graphene particles become more homogeneously when grinding speed was increased.
- Among to our results the structural characteristic was improved with increasing grinding speed.

Acknowledgement

This research was supported by Basic Science Research Program through the National Research

Foundation of Korea (NRF) funded by the Ministry of Education, Science and Technology (NRF-2011-0009022).

References

1. W. Wonsawat, S. Chuanuwatanakul, W. Dungchai, E. Punrat, S. Motomizu, and O. Chailapakul, 2012, "Graphene-carbon paste electrode for cadmium and lead ion monitoring in a flow-based system." Talanta, 100, pp. 282-289.
2. J. R. Potts, D. R. Dreyer, C. W. Bielawski, and R. S. Ruoff, 2011, "Graphene-based polymer nanocomposites." Polymer, Vol. 52, pp. 5-25.
3. W. Hong, Y. Xu, G. Lu, C. Li, and G. Shi, 2008, "Transparent graphene / PEDOT-PSS composite films as counter electrodes of dye-sensitized solar cells." Electrochemistry Communications, Vol. 10, pp. 1555-1558.
4. Y. Jin, M. Jia, M. Zhang, and Q. Wen, 2013, "Preparation of stable aqueous dispersion of graphene nanosheets and their electrochemical capacitive properties." Applied Surface Science, Vol. 264, pp. 787-793
5. G. Yue, J. Wu*, Y. Xiao, M. Huang, J. Lin, and L. F. Z. Lan, 2013, "Platinum/graphene hybrid film as a counter electrode for dye-sensitized solar cells." Electrochemical Acta, Vol. 92, pp. 64-70.
6. D. W. Zhang, X. D. Li, H. B. Li, S. Chen, Z. Sun, X. J. Yin, and S. M. Huang, 2011, "Graphene-based counter electrode for dye-sensitized solar cells." CARBON, Vol. 49, pp. 5382-5388.
7. A. Marinkas, F. Arena, J. Mitzel, G.¨ Nther, M. Prinz, A. Heinzel, V. Peinecke, and H. Natter, 2013, "Graphene as catalyst support: The influences of carbon additives and catalyst preparation methods on the performance of PEM fuel cells." CARBON, Vol. 58, pp. 139-150.
8. R. Zou, Z. Zhang, K. Xu, L. Jiang, Q. Tian, Y. Sun, Z. and Chen, J. Hu, 2012, "A method for joining individual graphene sheets." CARBON, Vol. 50, pp. 4965-4972.
9. Y. Zhang, S. Wang, L. Li, K. Zhang, J. Qiu, M. Davis, and L. J. Hope-Weeks, 2012, "Tuning electrical conductivity and surface area of chemically-exfoliated graphene through nanocrystal functionalization." Materials Chemistry and Physics, Vol. 135, pp. 1057-1063.
10. S. Wang, R. Liang, B. Wang and C. Zang, 2009, "Dsipersion and thermal conductivity of carbon nanotube composites." Carbon, Vol. 47, pp. 53-57.
11. Y. Yao and Ching–ping, 2012, ‘’Monolayer graphene growth using additional etching process in atmospheric pressure chemical vapor deposition’’, Carbon, Vol. 50, pp. 5203-5209.
12. H. Chung, M. Batmunkh, Y. G. Kim, S. Huh and H. M. Jeong, 2011, "Grinding and Dispersion Characteristics of Multi-Walled Carbon Nanotubes in Aqueous Solution." Applied Surface Science, 00, pp. 000-000.
13. T. Yamabe, M. Fujii, S. Mori, H. Kinoshita and S. Yata, 2004, "The structural analysis of various hydro–graphene species", Synthetic Metals, Vol. 145, pp. 31-36.
14. R. J. Seresht, M. Jahanshahi, A. Rashadi and A. A. Ghoreyshi, 2013, "Synthesize and characterization of graphene nanosheets with high surface area and nano–porous structure", Applied surface science, Vol. 276, pp. 672-681.
15. F. Liu and Y. Zhang, 2010, "Substrate–free synthesis of large area, continues multi-layer graphene film", Carbon, Vol. 48, pp. 2394-2400.